Report

Current Biology

Photosystems in the eye-like organelles of heterotrophic warnowiid dinoflagellates

Highlights

- High-coverage transcriptomic data are now available for five warnowiid genera
- Heterotrophic warnowiids retain a part of the ancestral photosynthetic mechanism
- Heterotrophs lack transcripts for PS II and Calvin cycle genes

Authors

Elizabeth C. Cooney, Corey C. Holt, Victoria K.L. Jacko-Reynolds, Brian S. Leander, Patrick J. Keeling

Correspondence

lizcooney22@gmail.com

In brief

Cooney et al. present a robust transcriptomic dataset for the warnowiid dinoflagellates, which are unique because they have an organelle similar to metazoan eyes. This dataset includes five different genera and reveals that heterotrophic taxa retain only part of the photosynthetic pathway, apparently lacking PS II and the Calvin cycle.

Cooney et al., 2023, Current Biology *33*, 4252–4260
October 9, 2023
https://doi.org/10.1016/j.cub.2023.08.052

CellPress

CellPress

Current Biology

Report

Photosystems in the eye-like organelles of heterotrophic warnowiid dinoflagellates

Elizabeth C. Cooney,[1,2,5,*] Corey C. Holt,[1,2] Victoria K.L. Jacko-Reynolds,[1] Brian S. Leander,[1,3] and Patrick J. Keeling[1,4]
[1]Department of Botany, University of British Columbia, Vancouver, BC V6T 1Z4, Canada
[2]Hakai Institute, Heriot Bay, BC V9W 5E3, Canada
[3]Department of Zoology, University of British Columbia, Vancouver, BC V6T 1Z4, Canada
[4]X (formerly Twitter): @pjkeelinglab
[5]Lead contact
*Correspondence: lizcooney22@gmail.com
https://doi.org/10.1016/j.cub.2023.08.052

SUMMARY

Warnowiid dinoflagellates contain a highly complex camera-eye-like structure called the ocelloid that is composed of different organelles resembling parts of metazoan eyes, including a modified plastid that serves as the retinal body.[1] The overall structure of the ocelloid has been investigated by microscopy; because warnowiids are not in culture and are rare in nature, we know little about their function.[1,2] Here, we generate single-cell transcriptomes from 18 warnowiid cells collected directly from the marine environment representing all 4 known genera and 1 previously undescribed genus, as well as 8 cells from a related lineage, the polykrikoids. Phylogenomic analyses show that photosynthesis was independently lost twice in warnowiids. Interestingly, the non-photosynthetic taxa still express a variety of photosynthesis-related proteins. *Nematodinium* and *Warnowia* (known or suspected to be photosynthetic[1,3]) unsurprisingly express a full complement of photosynthetic pathway components. However, non-photosynthetic genera with ocelloids were also found to express light-harvesting complexes, photosystem I, photosynthetic electron transport (PET), cytochrome b_6f, and, in *Erythropsidinium*, plastid ATPase, representing all major complexes except photosystem II and the Calvin cycle. This suggests that the non-photosynthetic retinal body has retained a reduced but still substantial photosynthetic apparatus that perhaps functions using cyclic electron flow (CEF). This may support ATP synthesis in a reduced capacity, but it is also possible that the photosystem has been co-opted to function as a light-driven proton pump at the heart of the sensory mechanism within the complex architecture of ocelloids.

RESULTS AND DISCUSSION

Cell collection and identification

Warnowiid dinoflagellates possess some of the most complex subcellular structures known. The most striking of these is the ocelloid—a miniature camera-eye-like structure composed of separate modified membrane-bound organelles resembling the iris, cornea, lens, and retina of multicellular metazoan eyes.[1,4] The retinal body of the ocelloid is a derived plastid containing tightly packed wave-form thylakoid membranes and is thought to have lost photosynthesis and been modified to serve a photosensory role. Although the structure of the ocelloid has been explored in detail,[1] its function in phototaxis remains speculative, as warnowiids are both rare and uncultured, limiting molecular data to a low-coverage survey of one species.[1,2,4,5] Similarly, there are no experimental data on a potential mechanism for light sensing, although it has been hypothesized to be rhodopsin-based.[2] Unfortunately, little is known about the diet and growth requirements of any warnowiids due to their rarity, making cultivation and subsequent experimentation unfeasible.

To create a molecular dataset for this group, we collected a total of 18 warnowiid cells from 5 different genera, as well as 8 related polykrikoid cells. All cells were easily recognizable in environmental samples due to their distinctive morphologies, and for most cells, known cellular characteristics could be unambiguously matched to molecular identification at the genus level using SSU and LSU rRNA genes from transcriptome data (Figure 1).[6,7] For example, *Nematodinium* cells were pigmented green (Figure 2; Video S1), whereas *Erythropsidinium* cells were pink, with a prominent piston-like appendage (Figures 2Q and 2R; Video S2). *Warnowia* cells were colorless, other than the dark ocelloid plastids at the midpoint of the cell, and bore a characteristically long cingulum encircling the anterior three quarters of the cell twice (Figures 2M–2P; Video S3). *Proterythropsis* morphology was more plastic (Figures 1 and 2A–2H; Video S4), requiring the use of SSU rRNA gene sequences for confident identification, but in SSU and LSU rRNA trees, they all branch together with strong support (Figure 1). *Polykrikos* cells were identified by their distinctive pseudocolonial body plan, characterized by interconnected zooids integrated into a single multinucleated cell (Figure S1; Video S5).[8,9] For all these genera, not surprisingly, variation among cells was observed, probably due to a mix of their representing different species (Figure 1), natural plasticity, and because several cells were found to have distinctive morphology because they were currently undergoing cell division (Figures 1 and 2; Videos S1–S6), but the

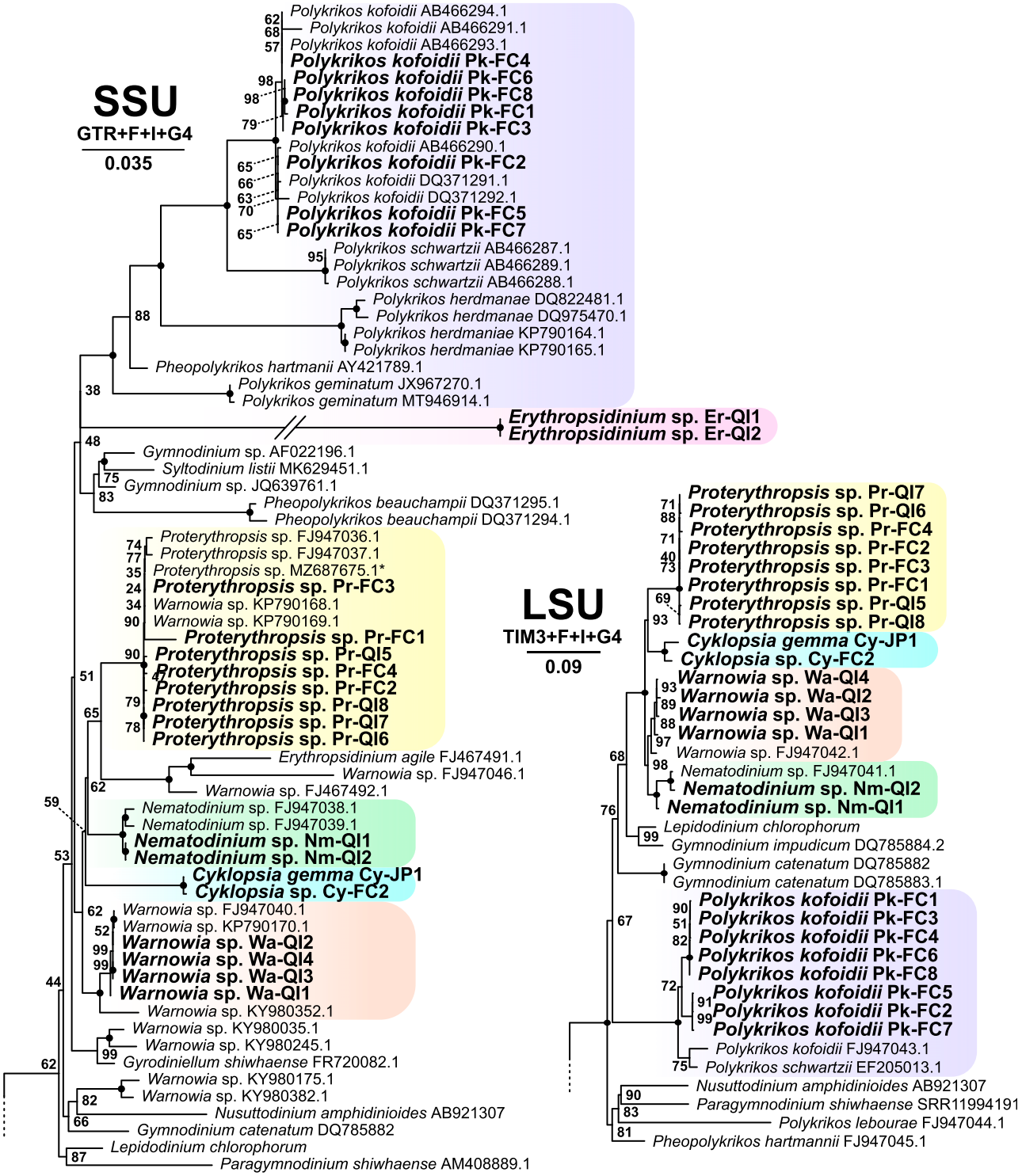

Figure 1. Maximum likelihood phylogenies of Gymnodiniales SSU and LSU rRNA gene sequences

Node values show bootstrap support, with values of 100 indicated by black circles. Sequences from cells isolated in the present study are in bold. Taxa denoted with an asterisk are truncated sequences. Scale bars indicate the number of nucleic acid substitutions per site and are accompanied by the substitution models used to infer each tree. Full trees and associated alignments can be found at https://doi.org/10.5061/dryad.nzs7h44vf.

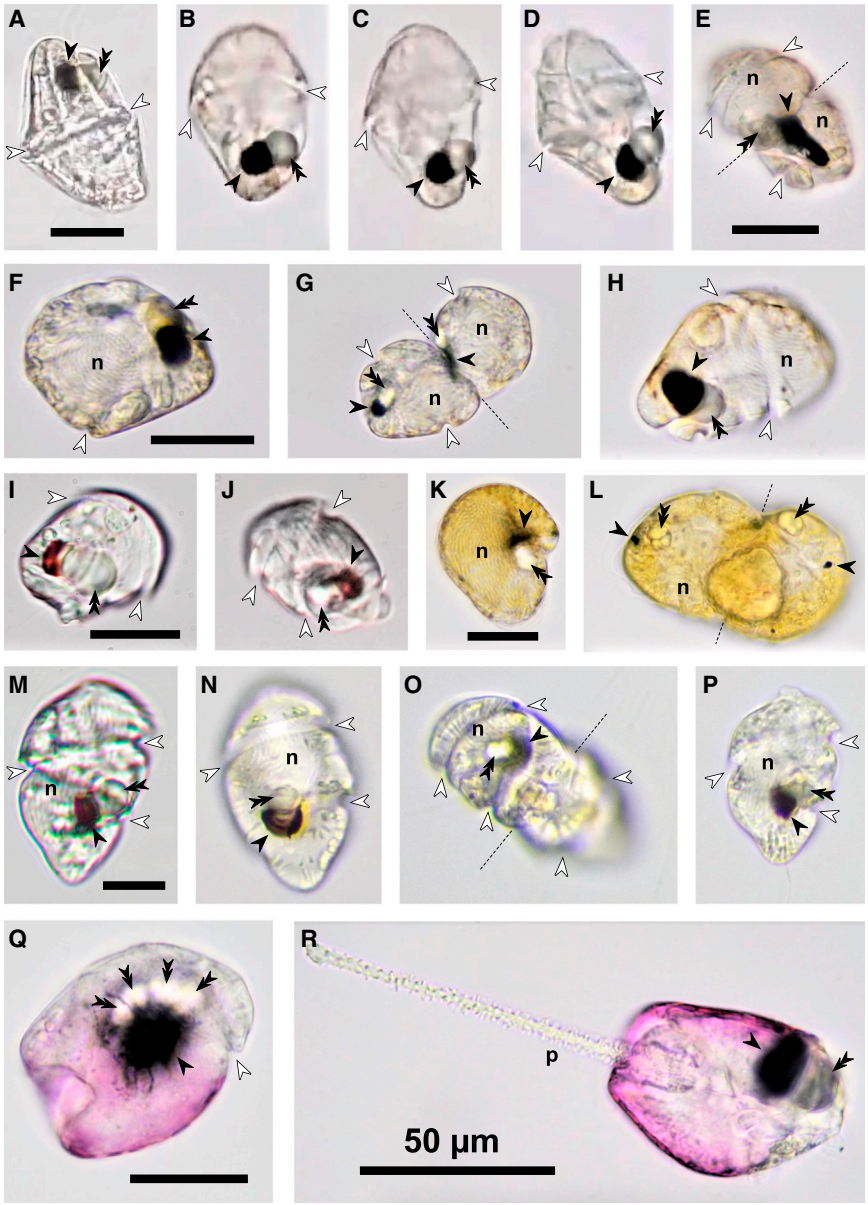

Figure 2. Light micrographs of warnowiid cells

(A–H) *Proterythropsis* sp. cells Pr-FC1:4 and Pr-QI5:8.

(I) *Cyklopsia gemma* gen. nov. sp. nov. cell Cy-JP1.

(J) *Cyklopsia* sp. cell Cy-FC2.

(K and L) *Nematodinium* sp. cells Nm-QI1 and Nm-QI2.

(M–P) *Warnowia* sp. cells Wa-QI1:4.

(Q and R) *Erythropsidinium* sp. cells Er-QI1 and Er-QI2.

Black single arrows, ocelloid retinal body; black double arrows, ocelloid hyalosome; white arrows, cingulum; n, nucleus; p, piston. Dotted lines depict the cleavage planes in dividing cells. Scale bars, 25 μm unless otherwise indicated. Scale bar in (A) applies to (A)–(D), (F) applies to (F)–(H), (I) applies to (I) and (J), (K) applies to (K) and (L), (M) applies to (M)–(P).

See also Figure S1.

consistency between overall morphology and their position in rRNA trees lends their genus-level identification strong support. All supplemental videos are available at https://doi.org/10.5281/zenodo.7269039.

Two cells clearly contained an ocelloid but did not match the characteristics of any known warnowiid genera, forming an independent branch within warnowiids in rRNA trees (Figure 1). We characterize these as a new genus, *Cyklopsia* gen. nov. (formal description with type species in Data S1). *Cyklopsia* cells shared a similar but not identical overall morphology; they are notably smaller than all other warnowiids in this study (Figures 2I and 2J), with proportionately large ocelloids, the retinal bodies of which are a uniquely translucent red color (Video S6). They appear to contain nematocyst-like extrusomes. The SSU and LSU rRNA gene sequences from these cells were also highly similar, but not identical, suggesting that they represent two species (Figure 1).

Transcriptome sequencing and phylogenomic analysis

Single-cell transcriptomes were prepared from each of the 26 individual cells. The quality of single-cell transcriptomes included in the multi-gene phylogenomic analysis varied, but in general, at least one cell from each genus yielded a transcriptome containing more than 50% of conserved genes in BUSCO v5 coverage estimates against the alveolata_odb10 database. *Nematodinium* was the exception, with the most complete transcriptome-producing coverage estimates of just under 30% (Table S1). In cases where cells produced very low yields (e.g., *Proterythropsis* cells Pr-FC1 and Pr-FC4), the genus was otherwise well-represented by other transcriptomes in the dataset.

In a maximum likelihood (ML) phylogeny inferred from an alignment of 222 conserved genes (53,387 sites), the cells fell into the same genus-level clusters as inferred from morphology and rRNA trees, and all relationships between warnowiid genera were resolved with full support (Figure 3). *Erythropsidinium* is sister to the rest of the warnowiids, which formed two additional groups: a clade consisting of *Nematodium*/*Warnowia* and a clade consisting of *Proterythropsis*/*Cyklopsia*. This strongly supported topology shows that photosynthesis was lost twice independently in warnowiids: once in the ancestor of *Erythropsidinium* and once in the ancestor of *Proterythropsis* and *Cyklopsia*. *Polykrikos kofoidii* cells all branched with the previously reported species, *Polykrikos lebouriae*,[10] but surprisingly, both ML and Bayesian analyses placed two other dinoflagellates, *Gymnodinium catenatum* and *Lepidodinium chlorophorum*, as a more immediate sister group to the warnowiid clade than the polykrikoids, with full support. This suggests that these more conventional and photosynthetic taxa are the closest

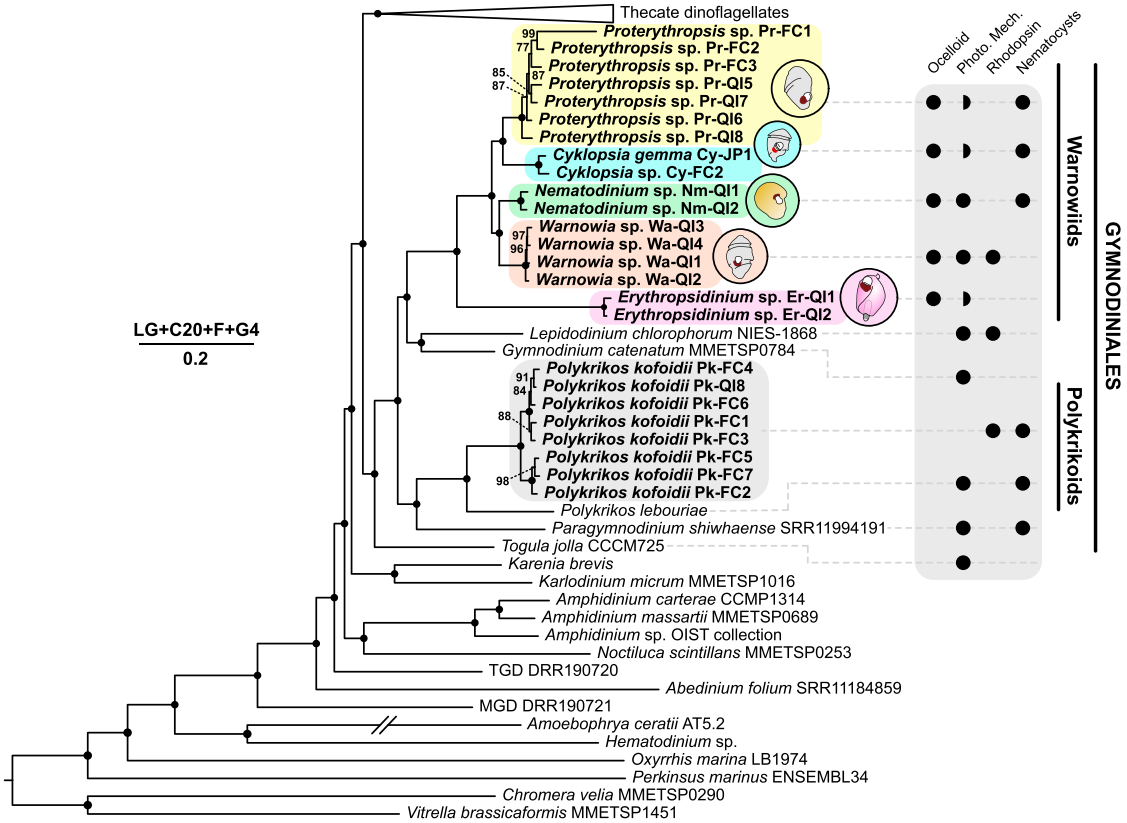

Figure 3. Maximum likelihood (ML) phylogeny of dinoflagellates inferred from an alignment of 222 conserved genes

Node values show bootstrap support, with values of 100 indicated by black circles at nodes. Cell sequences from the present study are bolded. Shortened branch is half its original length. Scale bar indicates the number of amino acid substitutions per site and is accompanied by the mixture model used to infer the tree. Presence of ocelloids, photosynthetic mechanisms (photo. mech.), rhodopsins, and nematocysts are mapped onto lineages, indicated by large, black-filled circles. Lineages missing PS II are indicated with a half circle. See also Table S1.

relatives to warnowiids, and because polykrikoids are the only other dinoflagellates with complex nematocysts similar to those found in some warnowiids, it also suggests that complex nematocysts have been lost both within the warnowiids and within their closest relatives.

Evidence for photosystems in the ocelloid retinal body

As most warnowiids lack visible photosynthetic pigment and possess sophisticated structures for predation, the majority of them have been assumed to be heterotrophic, and the ocelloid retinal body is by extension considered to be a non-photosynthetic plastid.[1,2,4,6] The clear exception to this is *Nematodinium*, which has distinct pigmented plastid regions as well as an ocelloid retinal body and is considered to be mixotrophic.[1] The genus *Warnowia* may also include photosynthetic members, as some have been reported to contain pigmented plastid-like structures.[3] The overlapping traits of some *Warnowia* and *Nematodinium* suggest that some photosynthetic plastid-bearing species can change the composition of plastids within the cell, sometimes appearing non-photosynthetic.[7] Moreover, a handful of photosynthesis-related genes have been reported from *Warnowia* and *Erythropsidinium*, and autofluorescence of the retinal body has also raised the question of whether these ostensibly heterotrophic cells might retain photosynthesis.[1,2]

We comprehensively identified genes involved in a wide range of photosynthetic functions across the entire known diversity of warnowiids (Figure 4). Transcripts for genes involved in all aspects of typical light harvesting, linear electron flow, and photosynthesis were not surprisingly found in *Nematodiumium* and *Warnowia*, confirming their proposed photosynthetic capabilities. For both lineages, the absences of transcripts for a few individual genes scattered among photosystems are most likely due to sampling errors stemming from transcriptome incompleteness (and especially low coverage in the case of *Nematodinium*). More surprisingly, however, heterotrophic warnowiids were also found to express genes for proteins involved in photosystem I (PS I), cytochrome b_6f (*petA*, *petB*, *petC*, and *petD*), plastoquinol-oxidizing plastid terminal oxidase (*PTOX*), electron transport (*petF* (*Fd*), *petH* (*FNR*), and *petJ*), and light-harvesting complexes (*FCP* and *PCP*). Transcripts for ATP synthase proteins (*atpA-atpI*) were also found in *Erythropsidinium*, but only a single gene (*atpF*) was found in both *Proterythropsis* and *Cyklopsia*; in both cases, the *atpF* was highly divergent (Figure S2). Overall, this suggests the possible loss of the ATP synthase complex as a whole in these taxa with *atpF* retained as a relic or in a derived form with a newly assumed function. This would mean that the complex was differentially retained in the two clades that lost photosynthesis independently.

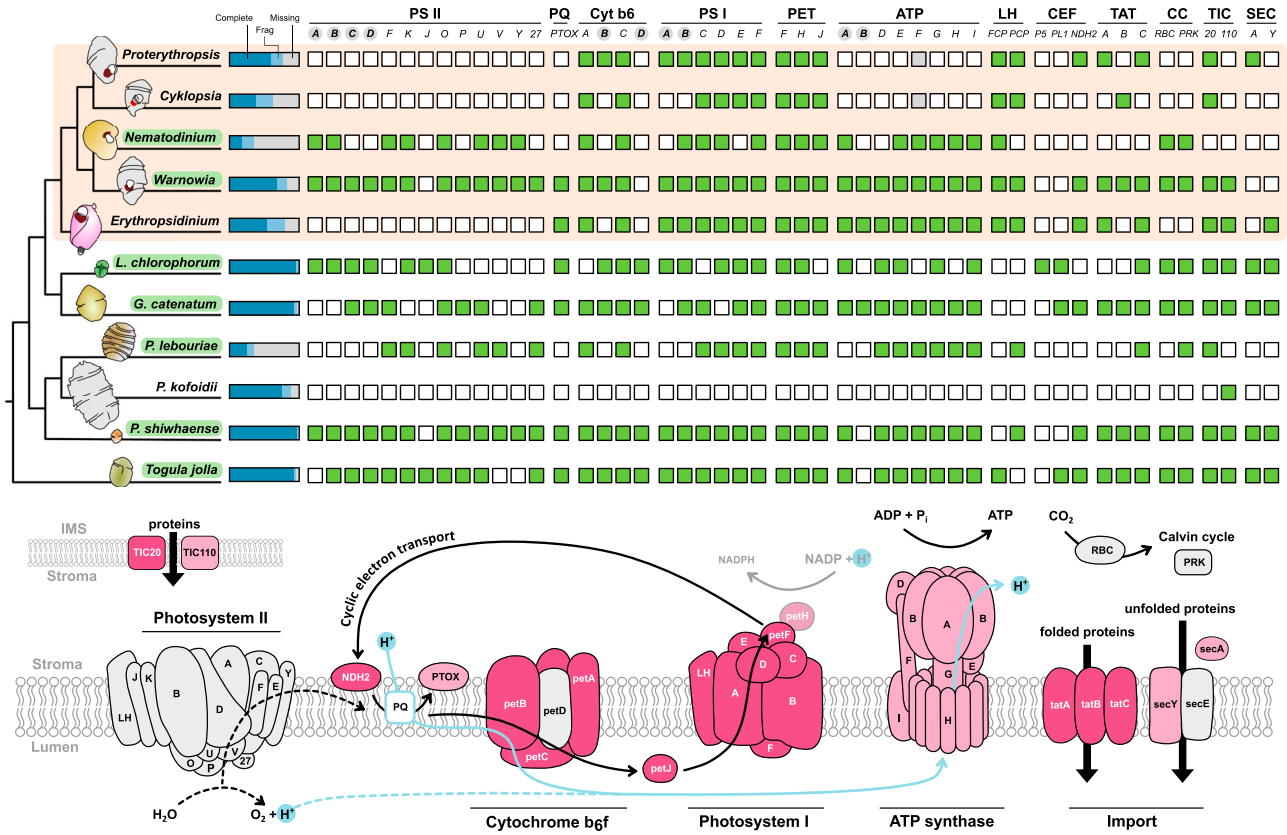

Figure 4. Schematic of photosynthesis-related gene transcripts in warnowiids and the greater Gymnodiniales clade

Top: cladogram shows the relationships between warnowiids and their relatives, with photosynthetic lineages highlighted in green. Bars adjacent to branches represent BUSCO coverage estimates (compared against alveolata_odb10) of all combined transcriptomes of each taxon, showing the proportion of complete, fragmented, and missing orthologs. Green and white squares indicate the presence and absence of plastid genes associated with the photosynthetic apparatus: photosystem II (PS II), plastoquinone pool (PQ), cytochrome b_6f (Cyt b6), photosystem I (PS I), photosynthetic electron transport (PET), ATP synthase (ATP), light harvesting (LH), cyclic electron flow (CEF), twin arginine translocation (TAT), Calvin cycle (CC), and translocons of the inner chloroplast membrane (TICs). PetF (ferredoxin) and PetH (ferredoxin-NADP(H) reductase) are also known as Fd and FNR, respectively. PetH (and associated NADPH production) is grayed to indicate the possible variability of its role in different plastids. Column headers for genes in PS II are shorthand for genes named *psbA-psb27*. Similarly, headers for genes in PS I are shorthand for *psa* prefixed gene names. *PTOX*, plastid terminal oxidase. Headers in Cyt b6 and PET are shorthand for *pet* prefixed gene names. For ATP headers, (A)–(E) ATP subunits alpha (*atpA*), beta (*atpB*), delta (*atpD*), and epsilon (*atpE*); (F) ATP subunit b (*atpF*). *FCP*, fucoxanthin chlorophyll binding protein; *PCP*, peridinin chlorophyll binding protein; *P5*, proton gradient regulation 5 (PGR5); *PL1*, PGR5-like protein 1; *NDH2*, type I NADH dehydrogenase complex. Headers under TAT are shorthand for *tatA-tatC*. *RBC*, ribulose-1,5-bisphosphate carboxylase-oxygenase or RuBisCo; *PRK*, phosphoribulokinase. Headers under TIC stand for *TIC20* and *TIC110*. Bolded column headers in gray circles indicate genes typically encoded in dinoflagellate plastid genomes. Bottom: schematic of the photosynthetic and other components present in typical photosynthetic dinoflagellates with those in heterotrophic warnowiids colored pink. Dark pink indicates proteins present in all heterotrophic warnowiids while light pink components are only found in *Erythropsidinium*. Thin, black arrows depict electron flow, with dotted lines showing the pathways likely absent in heterotrophic warnowiids. Blue arrows show the flow of protons and thick black arrows show the movement of proteins. Large membrane represents that of the thylakoid, while the smaller membrane represents the inner-most chloroplast membrane that separates the stroma from the intermembrane space (IMS).

See also Figures S2–S4.

Several of the photosynthesis-related genes found in the warnowiids are among the 12 typically encoded in plastid genomes of photosynthetic dinoflagellates. Among the non-truncated photosystem, cytochrome b_6f, and ATP synthase transcripts captured from warnowiids, those corresponding to typical plastid-encoded genes lacked N-terminal extensions, whereas the rest had characteristic plastid-targeting signal peptides (Figure S3). This is consistent with previous evidence that the warnowiid ocelloid has retained its plastid genome, but most photosynthesis-related genes are likely encoded in the nucleus and targeted post-translationally to the plastid as they are in other photosynthetic dinoflagellates.[1,11,12] In keeping with this, warnowiids also expressed the two chloroplast inner-membrane translocon genes known in dinoflagellates (*TIC20* and *TIC110*) and components of the twin arginine transporter pathway (*tatA-C*), confirming that they possess a mechanism for plastid protein import and a system for translocation of proteins into the thylakoid.[13–15] One sequence each of *secA* and *secY* were found in *Proterythropsis* and *Erythropsidinium*, respectively (*secE* was not found), suggesting that this alternative pathway for import of proteins into the thylakoid is also present but weakly expressed.[16] Because Tat and Sec pathways are responsible for the import of different proteins, respectively, the presence of both mechanisms suggests that thylakoid import in warnowiids is not particularly limited, even in heterotrophic taxa.

Of the genes known that could facilitate cyclic electron flow (CEF)—proton gradient regulation 5 (*PRG5*), PRG5-like protein 1 (*PRGL1*), and type II NADH dehydrogenase (*NDH2*)—*NDH2* was recovered in the warnowiids.[17,18] All taxa also expressed genes for plastid-targeted proteins relating to heme, isoprenoid, and iron-sulfur cluster biosynthetic pathways, which are typically retained in heterotrophic dinoflagellates even after photosynthesis is lost in the plastid (Figure S4).[18] Transcripts for petH, which may function in electron transfer from PS I, were present in all warnowiids.

Overall, the strongly prevailing pattern is that heterotrophic warnowiids are consistently missing transcripts for all photosystem II (PS II) and Calvin-cycle-specific components. Although it is possible that this is due to a lack of detection or the specific downregulation of these genes, neither of these explanations is compatible with the fact that the data come from multiple transcriptomes, many of them with deep coverage of other pathways in general and from multiple cells for each genus, collected at different times and under different conditions. The pattern of absence for these normally highly expressed genes correlates only with a single factor: the phylogenomic tree. The conclusion that these genes have been lost is bolstered by the clear pattern of presence/absence displayed by *Nematodinium*, *Warnowia*, and non-warnowiid lineages sampled in this study, where transcripts of PS II components were consistently found, even in *Nematodinium* transcriptomes with comparatively low coverage. In contrast, the non-photosynthetic polykrikoid transcriptomes consistently did not recover any putative photosynthesis-related genes, suggesting that the photosynthesis transcripts found in the warnowiids are unlikely to be false positives in the form of functionally divergent homologs. Although full genome sequencing is the only way to conclusively demonstrate the absence of an individual gene, the pattern of absence of large sets of highly conserved, highly expressed, and functionally related genes like in PS II is most simply explained by the loss of the complex.

A repurposed photosynthetic apparatus?

The presence of photosynthesis-related genes in all warnowiids raises the question of whether lineages assumed to be heterotrophic are in fact mixotrophs. However, without PS II or crucial Calvin cycle components, these cells should be incapable of CO_2 fixation. An alternative hypothesis is that PS II genes are present but downregulated. This photoacclimation strategy has been documented in some microalgae, including dinoflagellates, where decreasing the ratio of PS II to PS I leads to the cyclic flow of electrons (CEF) around PS I to temporarily reduce reactive oxygen species (ROS) from PS II activity that induce cellular damage.[19–21] The symbiotic dinoflagellate *Symbiodinium* is thought to employ CEF in response to temperature change in coral hosts, as several strains have been shown to increase PS I activity under warming conditions.[22] The Ross Sea dinoflagellate (RSD) has also been shown to use CEF in its haptophyte kleptoplasts, as PS II activity has been shown to decrease in the plastids it steals.[18,23] In this case, however, CEF is hypothesized to be used not as protection from ROS but instead because acquiring PS II requires the transfer of seven genes from its food alga, whereas only two are needed to use PS I and CEF.[18]

The situation in RSD is very different from that in warnowiids because warnowiid photosynthesis genes are not recently acquired but instead descend from the ancestral peridinin-type plastid. The absence of PS II transcripts must therefore be the result of loss or downregulation.[1] Downregulation is, similar to sampling error, unlikely to explain the consistent pattern across so many individual cells collected from different genera, times, and locations because in other species that use downregulation of PS II (e.g., *Symbiodinium*), it is a temporary physiological reaction to light stress. Overall, the consistent pattern of PS II absence in warnowiids is more consistent with the irreversible loss of the entire complex. Based on the phylogenetic position of *Nematodinium* and *Warnowia*, the putative loss of PS II and the Calvin cycle must have occurred twice independently in *Erythropsidinium* and the common ancestor of *Cyklopsia* and *Proterythropsis*. This also presents the possibility that there are differences between the plastid biology of these two lineages, possibly including ATP synthase components that were almost universally present in *Erythropsidinium* but absent in *Cyklopsia* and *Proterythropsis*, with the exception of the divergent *atpF*. As with PS II, ATP synthase expression can be diminished in conditions of high light stress or nutrient-poor conditions, neither of which is likely to have occurred uniformly across the cells collected in this study.[24–27] How a proton gradient would be utilized in the absence of the ATPase complex is not clear, but diverse symporters also use proton gradients and are likely alternatives.

Few mechanistic advantages have been proposed in cases of either the loss or the downregulation of PS II other than the reduction of oxidative stress. Although CEF around PS I can provide a source of ATP, the lack of ATP synthase expression in *Cyklopsia* and *Proterythropsis* is inconsistent with this mechanism.[28] As the loss of both PS II and ribulose-1,5-bisphosphate carboxylase (RuBisCo) has been confirmed in the uncultivated nitrogen-fixing cyanobacterium UCYN-A, this reduction may also create more favorable conditions for nitrogen fixation.[29,30] However, in warnowiids, there is no evidence for this. Instead, the fact that this rare configuration is associated with the highly modified and singularly unique ocelloid raises the intriguing possibility that warnowiids have repurposed the photosynthetic apparatus to perform a sensory role using cyclic electron transport.

If the ocelloid is a light-sensing organelle complex, then the retinal body most likely uses light to create an ion gradient to initiate a sensory transduction cascade. Previously, the photoactive protein rhodopsin has been hypothesized to play this role because proton-pumping proteorhodopsin has been reported in *Erythropsidinium*.[2] We found proteorhodopsin and retinal synthesis (*diox1*) transcripts in *Warnowia*, but not in any heterotroph (Figure S4). Moreover, rhodopsins have never been shown to localize to the inside of the retinal body or indeed into any plastid in any eukaryote, and the sequences we recovered from *Warnowia* lack an N-terminal plastid-targeting extension.[31] This all makes rhodopsins unlikely candidates for a plastid proton pump. However, this may not be that surprising when one considers that the plastid is already home to a well-known light-driven proton pump: the photosystems. Indeed, inserting a second proton pump into the same membrane as the photosystems might be physiologically harmful, since it would create potential problems for regulating both systems independently. Overall, we propose a much simpler explanation that the plastid adopted a sensory role not by gaining new functions but rather by repurposing the pre-existing gradient-inducing transmembrane system already present in cytochrome

b_6f and PS I; this system could take on a sensory role in the ocelloid simply by coupling it with a downstream proton-driven signal transduction mechanism that detects either an excess of ions in the thylakoid lumen or a paucity of ions in the stroma. Although this might seem like a radical functional shift for photosystems, it is substantially simpler than proposing the plastid had to be invaded by another light-driven proton pump when one already exists, which importantly is also inconsistent with the transcriptomic data.

It must be pointed out that no signal transduction mechanisms have been described in this lineage, and indeed, the sensory role of the ocelloid may have been misinterpreted altogether. This needs to be tested experimentally (perhaps requiring cultivation), but the strong resemblance of the ocelloid to camera eyes in animals and the many examples of much simpler eye spots used by many other lineages of protist (including other dinoflagellates) together make this the most likely function of the organelle, perhaps with ATP production as a secondary byproduct in some lineages.

The expansion of warnowiid molecular data has allowed us to resolve the relationships between and around these taxa and provides a data pool for future exploration into the unique biology of this group. In this vein, we present evidence that the ocelloid plastid retains and uses a subset of the ancestral photosynthetic apparatus, perhaps by utilizing CEF. The apparent absence of RuBisCo and the Calvin cycle suggests that the remaining components are used for something other than photosynthesis, which would add to a growing list of oddities that characterize this group.

STAR★METHODS

Detailed methods are provided in the online version of this paper and include the following:

- KEY RESOURCES TABLE
- RESOURCE AVAILABILITY
  - Lead contact
  - Materials availability
  - Data and code availability
- EXPERIMENTAL MODEL AND STUDY PARTICIPANT DETAILS
- METHOD DETAILS
  - Sequencing and transcriptome assembly
  - Identification and phylogenomic analysis
  - Plastid protein search
- QUANTIFICATION AND STATISTICAL ANALYSIS

SUPPLEMENTAL INFORMATION

Supplemental information can be found online at https://doi.org/10.1016/j.cub.2023.08.052.

ACKNOWLEDGMENTS

We thank Elisabeth Hehenberger for access to her annotated bacterial database and her advice. Thanks also to the Tula Foundation's Hakai Institute for its accommodations and support. This work was supported by grants from the Gordon and Betty Moore Foundation to P.J.K. (GBMF9201) and the Natural Sciences and Engineering Research Council of Canada to B.S.L. (NSERC 2019-03986) and P.J.K. (NSERC 2019-03994).

AUTHOR CONTRIBUTIONS

E.C.C. and P.J.K. conceptualized and wrote the original draft, with P.J.K. as project administrator. Investigation and visualization were performed by E.C.C., with assistance in methodology design from C.C.H. and V.K.L.J.-R. P.J.K. and B.S.L. acquired funding and supervised the project. Review and editing of the manuscript were performed by all authors.

DECLARATION OF INTERESTS

The authors declare no competing interests.

INCLUSION AND DIVERSITY

One or more of the authors of this paper self-identifies as an underrepresented ethnic minority in their field of research or within their geographical location. One or more of the authors of this paper self-identifies as a gender minority in their field of research. One or more of the authors of this paper self-identifies as a member of the LGBTQIA+ community. One or more of the authors of this paper received support from a program designed to increase minority representation in their field of research.

Received: June 6, 2023
Revised: August 3, 2023
Accepted: August 16, 2023
Published: September 12, 2023

REFERENCES

1. Gavelis, G.S., Hayakawa, S., White, R.A., Gojobori, T., Suttle, C.A., Keeling, P.J., and Leander, B.S. (2015). Eye-like ocelloids are built from different endosymbiotically acquired components. Nature *523*, 204–207. https://doi.org/10.1038/nature14593.
2. Hayakawa, S., Takaku, Y., Hwang, J.S., Horiguchi, T., Suga, H., Gehring, W., Ikeo, K., and Gojobori, T. (2015). Function and evolutionary origin of unicellular camera-type eye structure. PLoS One *10*, e0118415. https://doi.org/10.1371/journal.pone.0118415.
3. Hulburt, E.M. (1957). The taxonomy of unarmored Dinophyceae of shallow embayments on Cape Cod, Massachusetts. Biol. Bull. *112*, 196–219.
4. Greuet, C. (1977). Evolution structurale et ultrastructurale de l'ocelloide d'*Erythropsidinium pavillardi* Kofoid et Swezy (Peridinien Warnowiidae Lindemann) au cours des divisions binaire et palintomiques. Protistologica *13*, 127–143.
5. Gómez, F. (2017). The function of the ocelloid and piston in the dinoflagellate *Erythropsidinium* (Gymnodiniales, Dinophyceae). J. Phycol. *53*, 629–641. https://doi.org/10.1111/jpy.12525.
6. Gómez, F., López-García, P., and Moreira, D. (2009). Molecular phylogeny of the ocelloid-bearing dinoflagellates *Erythropsidinium* and *Warnowia* (Warnowiaceae, Dinophyceae). J. Eukaryot. Microbiol. *56*, 440–445. https://doi.org/10.1111/j.1550-7408.2009.00420.x.
7. Hoppenrath, M., Bachvaroff, T.R., Handy, S.M., Delwiche, C.F., and Leander, B.S. (2009). Molecular phylogeny of ocelloid-bearing dinoflagellates (Warnowiaceae) as inferred from SSU and LSU rDNA sequences. BMC Evol. Biol. *9*, 116. https://doi.org/10.1186/1471-2148-9-116.
8. Bütschli, O. (1873). Einiges fiber infusorien. Arch. Mikr. Anat. *9*, 657–678.
9. Hoppenrath, M., and Leander, B.S. (2007). Character evolution in polykrikoid dinoflagellates. J. Phycol. *43*, 366–377. https://doi.org/10.1111/j.1529-8817.2007.00319.x.
10. Gavelis, G.S., Wakeman, K.C., Tillmann, U., Ripken, C., Mitarai, S., Herranz, M., Özbek, S., Holstein, T., Keeling, P.J., and Leander, B.S. (2017). Microbial arms race: ballistic "nematocysts" in dinoflagellates represent a new extreme in organelle complexity. Sci. Adv. *3*, e1602552. https://doi.org/10.1126/sciadv.1602552.
11. Barbrook, A.C., and Howe, C.J. (2000). Minicircular plastid DNA in the dinoflagellate *Amphidinium operculatum*. Mol. Gen. Genet. *263*, 152–158. https://doi.org/10.1007/s004380050042.

12. Gabrielsen, T.M., Minge, M.A., Espelund, M., Tooming-Klunderud, A., Patil, V., Nederbragt, A.J., Otis, C., Turmel, M., Shalchian-Tabrizi, K., Lemieux, C., et al. (2011). Genome evolution of a tertiary dinoflagellate plastid. PLoS One *6*, e19132. https://doi.org/10.1371/journal.pone.0019132.

13. Hehenberger, E., Imanian, B., Burki, F., and Keeling, P.J. (2014). Evidence for the retention of two evolutionary distinct plastids in dinoflagellates with diatom endosymbionts. Genome Biol. Evol. *6*, 2321–2334. https://doi.org/10.1093/gbe/evu182.

14. Waller, R.F., and Kořený, L. (2017). Plastid complexity in dinoflagellates: a picture of gains, losses, replacements and revisions. Adv. Bot. Res. *84*, 105–143. https://doi.org/10.1016/bs.abr.2017.06.004.

15. Gould, S.B. (2008). Ariadne's thread: guiding a protein across five membranes in cryptophytes(1). J. Phycol. *44*, 23–26. https://doi.org/10.1111/j.1529-8817.2007.00437.x.

16. Albiniak, A.M., Baglieri, J., and Robinson, C. (2012). Targeting of lumenal proteins across the thylakoid membrane. J. Exp. Bot. *63*, 1689–1698. https://doi.org/10.1093/jxb/err444.

17. Peltier, G., Aro, E.M., and Shikanai, T. (2016). NDH-1 and NDH-2 plastoquinone reductases in oxygenic photosynthesis. Annu. Rev. Plant Biol. *67*, 55–80. https://doi.org/10.1146/annurev-arplant-043014-114752.

18. Hehenberger, E., Gast, R.J., and Keeling, P.J. (2019). A kleptoplastidic dinoflagellate and the tipping point between transient and fully integrated plastid endosymbiosis. Proc. Natl. Acad. Sci. USA *116*, 17934–17942. https://doi.org/10.1073/pnas.1910121116.

19. Niyogi, K.K. (1999). Photoprotection revisited: genetic and molecular approaches. Annu. Rev. Plant Physiol. Plant Mol. Biol. *50*, 333–359. https://doi.org/10.1146/annurev.arplant.50.1.333.

20. Finazzi, G., Barbagallo, R.P., Bergo, E., Barbato, R., and Forti, G. (2001). Photoinhibition of *Chlamydomonas reinhardtii* in State 1 and State 2: damages to the photosynthetic apparatus under linear and cyclic electron flow. J. Biol. Chem. *276*, 22251–22257. https://doi.org/10.1074/jbc.M011376200.

21. Davis, M.C., Fiehn, O., and Durnford, D.G. (2013). Metabolic acclimation to excess light intensity in *Chlamydomonas reinhardtii*. Plant Cell Environ. *36*, 1391–1405. https://doi.org/10.1111/pce.12071.

22. Aihara, Y., Takahashi, S., and Minagawa, J. (2016). Heat induction of cyclic electron flow around photosystem I in the symbiotic dinoflagellate *Symbiodinium*. Plant Physiol. *171*, 522–529. https://doi.org/10.1104/pp.15.01886.

23. Stamatakis, K., Vayenos, D., Kotakis, C., Gast, R.J., and Papageorgiou, G.C. (2017). The extraordinary longevity of kleptoplasts derived from the Ross Sea haptophyte *Phaeocystis antarctica* within dinoflagellate host cells relates to the diminished role of the oxygen-evolving photosystem II and to supplementary light harvesting by mycosporine-like amino acid/s. Biochim. Biophys. Acta Bioenerg. *1858*, 189–195. https://doi.org/10.1016/j.bbabio.2016.12.002.

24. Kanazawa, A., Ostendorf, E., Kohzuma, K., Hoh, D., Strand, D.D., Sato-Cruz, M., Savage, L., Cruz, J.A., Fisher, N., Froehlich, J.E., et al. (2017). Chloroplast ATP synthase modulation of the thylakoid proton motive force: implications for photosystem I and photosystem II photoprotection. Front. Plant Sci. *8*, 719. https://doi.org/10.3389/fpls.2017.00719.

25. Kohzuma, K., Froehlich, J.E., Davis, G.A., Temple, J.A., Minhas, D., Dhingra, A., Cruz, J.A., and Kramer, D.M. (2017). The role of light–dark regulation of the chloroplast ATP synthase. Front. Plant Sci. *8*, 1248. https://doi.org/10.3389/fpls.2017.01248.

26. Jean, N., Perié, L., Dumont, E., Bertheau, L., Balliau, T., Caruana, A.M.N., Amzil, Z., Laabir, M., and Masseret, E. (2022). Metal stresses modify soluble proteomes and toxin profiles in two Mediterranean strains of the distributed dinoflagellate *Alexandrium pacificum*. Sci. Total Environ. *818*, 151680. https://doi.org/10.1016/j.scitotenv.2021.151680.

27. Liu, Y., Chen, T., Wang, X., Song, S., and Li, C. (2020). Variation in the photosynthetic activities of the dinoflagellate *Akashiwo sanguinea* during formation of resting cysts. Mar. Biol. *167*, 1–12. https://doi.org/10.1007/s00227-020-03774-y.

28. Larkum, A.W.D., Szabó, M., Fitzpatrick, D., and Raven, J.A. (2017). Cyclic electron flow in cyanobacteria and eukaryotic algae. In Photosynthesis and Bioenergetics (World Scientific Publishing), pp. 305–344. https://doi.org/10.1142/9789813230309_0014.

29. Zehr, J.P., Bench, S.R., Carter, B.J., Hewson, I., Niazi, F., Shi, T., Tripp, H.J., and Affourtit, J.P. (2008). Globally distributed uncultivated oceanic N2-fixing cyanobacteria lack oxygenic photosystem II. Science *322*, 1110–1112. https://doi.org/10.1126/science.1165340.

30. Tripp, H.J., Bench, S.R., Turk, K.A., Foster, R.A., Desany, B.A., Niazi, F., Affourtit, J.P., and Zehr, J.P. (2010). Metabolic streamlining in an open-ocean nitrogen-fixing cyanobacterium. Nature *464*, 90–94. https://doi.org/10.1038/nature08786.

31. Patron, N.J., Waller, R.F., Archibald, J.M., and Keeling, P.J. (2005). Complex protein targeting to dinoflagellate plastids. J. Mol. Biol. *348*, 1015–1024. https://doi.org/10.1016/j.jmb.2005.03.030.

32. Picelli, S., Faridani, O.R., Björklund, A.K., Winberg, G., Sagasser, S., and Sandberg, R. (2014). Full-length RNA-seq from single cells using Smart-seq2. Nat. Protoc. *9*, 171–181. https://doi.org/10.1038/nprot.2014.006.

33. Martin, M. (2011). Cutadapt removes adapter sequences from high-throughput sequencing reads. EMBnet J. *17*, 10–12.

34. Bankevich, A., Nurk, S., Antipov, D., Gurevich, A.A., Dvorkin, M., Kulikov, A.S., Lesin, V.M., Nikolenko, S.I., Pham, S., Prjibelski, A.D., et al. (2012). SPAdes: a new genome assembly algorithm and its applications to single-cell sequencing. J. Comput. Biol. *19*, 455–477. https://doi.org/10.1089/cmb.2012.0021.

35. Altschul, S.F., Gish, W., Miller, W., Myers, E.W., and Lipman, D.J. (1990). Basic local alignment search tool. J. Mol. Biol. *215*, 403–410.

36. Katoh, K., and Standley, D.M. (2013). MAFFT multiple sequence alignment software version 7: improvements in performance and usability. Mol. Biol. Evol. *30*, 772–780. https://doi.org/10.1093/molbev/mst010.

37. Capella-Gutiérrez, S., Silla-Martínez, J.M., and Gabaldón, T. (2009). trimAl: a tool for automated alignment trimming in large-scale phylogenetic analyses. Bioinformatics *25*, 1972–1973. https://doi.org/10.1093/bioinformatics/btp348.

38. Nguyen, L.T., Schmidt, H.A., Von Haeseler, A., and Minh, B.Q. (2015). IQ-TREE: a fast and effective stochastic algorithm for estimating maximum-likelihood phylogenies. Mol. Biol. Evol. *32*, 268–274. https://doi.org/10.1093/molbev/msu300.

39. Roure, B., Rodriguez-Ezpeleta, N., and Philippe, H. (2007). SCaFoS: a tool for selection, concatenation and fusion of sequences for phylogenomics. BMC Evol. Biol. *7*, S2. Suppl 1. https://doi.org/10.1186/1471-2148-7-S1-S2.

40. Lartillot, N., Lepage, T., and Blanquart, S. (2009). PhyloBayes 3: a Bayesian software package for phylogenetic reconstruction and molecular dating. Bioinformatics *25*, 2286–2288. https://doi.org/10.1093/bioinformatics/btp368.

41. Haas, B.J., Papanicolaou, A., Yassour, M., Grabherr, M., Blood, P.D., Bowden, J., Couger, M.B., Eccles, D., Li, B., Lieber, M., et al. (2013). De novo transcript sequence reconstruction from RNA-seq using the Trinity platform for reference generation and analysis. Nat. Protoc. *8*, 1494–1512. https://doi.org/10.1038/nprot.2013.084.

42. Simão, F.A., Waterhouse, R.M., Ioannidis, P., Kriventseva, E.V., and Zdobnov, E.M. (2015). BUSCO: assessing genome assembly and annotation completeness with single-copy orthologs. Bioinformatics *31*, 3210–3212. https://doi.org/10.1093/bioinformatics/btv351.

43. Rambaut, A. (2007). FigTree, a graphical viewer of phylogenetic trees. http://tree.bio.ed.ac.uk/software/figtree/.

44. Almagro Armenteros, J.J.A., Tsirigos, K.D., Sønderby, C.K., Petersen, T.N., Winther, O., Brunak, S., von Heijne, G., and Nielsen, H. (2019). SignalP 5.0 improves signal peptide predictions using deep neural networks. Nat. Biotechnol. *37*, 420–423. https://doi.org/10.1038/s41587-019-0036-z.

45. Kolisko, M., Boscaro, V., Burki, F., Lynn, D.H., and Keeling, P.J. (2014). Single-cell transcriptomics for microbial eukaryotes. Curr. Biol. *24*, R1081–R1082. https://doi.org/10.1016/j.cub.2014.10.026.

46. Laetsch, D.R., Blaxter, M.L., and Leggett, R.M. (2017). BlobTools: interrogation of genome assemblies [version 1; peer review: 2 approved with reservations]. F1000Res. *6*, 1287.

47. Poux, S., Arighi, C.N., Magrane, M., Bateman, A., Wei, C.H., Lu, Z., Boutet, E., Bye-A-Jee, H., Famiglietti, M.L., Roechert, B., et al. (2017). On expert curation and scalability: UniProtKB/Swiss-Prot as a case study. Bioinformatics *33*, 3454–3460. https://doi.org/10.1093/bioinformatics/btx439.

48. Kalyaanamoorthy, S., Minh, B.Q., Wong, T.K.F., Von Haeseler, A., and Jermiin, L.S. (2017). ModelFinder: fast model selection for accurate phylogenetic estimates. Nat. Methods *14*, 587–589. https://doi.org/10.1038/nmeth.4285.

49. Hoang, D.T., Chernomor, O., Von Haeseler, A., Minh, B.Q., and Vinh, L.S. (2018). UFBoot2: improving the ultrafast bootstrap approximation. Mol. Biol. Evol. *35*, 518–522. https://doi.org/10.1093/molbev/msx281.

50. Burki, F., Kaplan, M., Tikhonenkov, D.V., Zlatogursky, V., Minh, B.Q., Radaykina, L.V., Smirnov, A., Mylnikov, A.P., and Keeling, P.J. (2016). Untangling the early diversification of eukaryotes: a phylogenomic study of the evolutionary origins of Centrohelida, Haptophyta and Cryptista. Proc. Biol. Sci. *283*, 1–10.

51. Ruch, S., Beyer, P., Ernst, H., and Al-Babili, S. (2005). Retinal biosynthesis in Eubacteria: in vitro characterization of a novel carotenoid oxygenase from *Synechocystis* sp. PCC 6803. Mol. Microbiol. *55*, 1015–1024. https://doi.org/10.1111/j.1365-2958.2004.04460.x.

STAR★METHODS

KEY RESOURCES TABLE

REAGENT or RESOURCE	SOURCE	IDENTIFIER
Chemicals, peptides, and recombinant proteins		
Triton X-100	Sigma-Aldrich	cat. no. T9284
dNTP mix	ThermoFisher	cat. no. R0192
First-strand buffer	ThermoFisher	cat. no. 18064-014
Superscript II reverse transcriptase	ThermoFisher	cat. no. 18064-014
Recombinant Ribonuclease Inhibitor	ThermoFisher	cat. no. 10777019
Betaine	Sigma-Aldrich	cat. no. B0300
Magnesium chloride	Sigma-Aldrich	cat. no. M8266
KAPA HiFi HotStart ReadyMix (2x)	Fisher Scientific	cat. no. 50-196-5299
Ampure XP beads	ThermoFisher	cat. no. Q32854
UltraPure DNase/RNase-Free Distilled Water	ThermoFisher	cat. no. 10977023
Ethyl alcohol anhydrous	Greenfield Global	cat. no. P006EAAN
DTT	Thermofisher	cat. no. 18064-014
Critical commercial assays		
Nextera XT	Illumina	FC-131-1024
Nextera	Illumina	FC-131-1024
Deposited data		
Raw sequencing reads	This paper	NCBI SRA: PRJNA922587
SSU sequences	This paper	GenBank: OP604718-OP604743
LSU sequences	This paper	GenBank: OP604692-OP604717
Experimental models: Organisms/strains		
Proterythropsis sp.	This paper	N/A
Nematodinium sp.	This paper	N/A
Warnowia sp.	This paper	N/A
Erythropsidinium sp.	This paper	N/A
Cyklopsia gemma	This paper	N/A
Cyklopsia sp.	This paper	N/A
Polykrikos kofoidii	This paper	N/A
Oligonucleotides		
Oligo-dT30VN (50–AAGCAGTGGTATCAACGCAGAGTACT30VN-30)	Picelli et al.[32]	N/A
IS-PCR oligo (50-AAGCAGTGGTATCAACGCAGAGT-30)	Picelli et al.[32]	N/A
TSO (50-AAGCAGTGGTATCAACGCAGAGT ACATrGrG+G-30)	Picelli et al.[32]	N/A
Software and algorithms		
Cutadapt	Martin[33]	http://code.google.com/p/cutadapt/

(*Continued on next page*)

Continued

REAGENT or RESOURCE	SOURCE	IDENTIFIER
rnaSPAdes	Bankevich et al.[34]	http://bioinf.spbau.ru/spades
BLAST	Altschul et al.[35]	https://blast.ncbi.nlm.nih.gov/
MAFFT	Katoh and Standley[36]	https://mafft.cbrc.jp/alignment/software/
trimAl	Capella-Gutiérrez et al.[37]	http://trimal.cgenomics.org/
IQ-Tree	Nguyen et al.[38]	http://www.iqtree.org/
SCaFoS	Roure et al.[39]	http://megasun.bch.umontreal.ca/Software/scafos/ scafos.html
Phylobayes	Lartillot et al.[40]	http://www.atgc-montpellier.fr/phylobayes/
Transdecoder	Haas et al.[41]	https://github.com/TransDecoder/TransDecoder/wiki
BUSCO	Simão et al.[42]	https://busco.ezlab.org
FigTree	Rambaut[43]	https://beast.community/figtre
SignalP	Almagro Armenteros et al.[44]	http://www.cbs.dtu.dk/services/SignalP/

RESOURCE AVAILABILITY

Lead contact

Requests for further information, resources, and reagents can be directed to and will be fulfilled by the lead contact, Elizabeth Cooney (lizcooney22@gmail.com).

Materials availability

This study did not generate new unique reagents.

Data and code availability

- Transcriptome sequencing reads have been deposited in the NCBI Short Read Archive (SRA): PRJNA922587 and are publicly available as of the date of publication. Accession numbers are listed in the key resources table.
- This paper does not report original code.
- Any additional information required to reanalyze the data reported in this paper is available from the lead contact upon request.

EXPERIMENTAL MODEL AND STUDY PARTICIPANT DETAILS

All sample collections were conducted along the shorelines of English Bay in Vancouver and the Hakai Quadra Island Ecological Observatory in British Columbia from May 2020 to July 2022. Net tows (20 μm mesh) were deployed from public boat docks at Snauq (False Creek) and Jericho Beach Pier, and from a rocky outcropping on Quadra Island. Specific dates and locations for each sample can be found in Table S1. After each collection, samples were viewed under a Leica DM IL microscope within an hour to search for interesting and understudied dinoflagellate taxa. *Proterythropsis* sp., *Cyklopsia* spp., *Nematodinium* sp., *Warnowia* sp., *Erythropsidinium* sp., and *Polykrikos kofoidii* cells were isolated from samples using a microcapillary pipet and washed with water that had been syringe filtered (0.2 μm) from the corresponding sample. Each cell was imaged (stills and video) using a Sony A7r III and then placed into lysis buffer.[32] Isolated cells were stored at -70°C until cDNA extraction.

METHOD DETAILS

Sequencing and transcriptome assembly

Extraction of mRNA and synthesis of cDNA for each sample was performed according to the Smart-seq2 protocol.[32,45] Libraries were prepared at the Sequencing and Bioinformatics Consortium, University of British Columbia, and sequenced on the Nextseq platform

(raw data: SRA project PRJNA922587). Trimming of forward and reverse raw reads was performed using Cutadapt before assembly with rnaSPAdes v3.15.1.[33,34] Decontamination of each assembly was achieved by using BLASTx and BLASTn to search NCBI nt and Uniprot (The Uniprot Consortium 2021) reference databases respectively to remove bacterial, metazoan, diatom, and sequences from other taxa that had been observed in the environmental samples.[38] Contaminants were identified for removal using BlobTools.[46] Nucleotide transcriptomes were translated to peptides using TransDecoder v5.5.0 (https://github.com/TransDecoder/TransDecoder/wiki) for open reading frame identification and annotation and BLASTP to search with an e-value threshold of $\leq$ 1e10^{-5} against the Uniprot database.[47] All assemblies are available at https://doi.org/10.5061/dryad.nzs7h44vf.

Identification and phylogenomic analysis

Cells could be taxonomically identified to the genus level based on morphology with the exception of Cy-JP1, and Cy-FC2. The most complete sequences for SSU and LSU rRNA genes (Genbank accession numbers OP604692-OP604743) were extracted from each transcriptome using BLASTn and submitted as queries in megaBLAST searches against Genbank to confirm these identities. Sequences were combined with curated collections of dinoflagellate SSU and LSU sequence data, aligned with MAFFT v.7.48, trimmed at a 30% gap threshold with trimAl v.3 and trees were inferred for each gene alignment using IQ-TREE v1.6.12.[36–38] Trees were generated using the ultrafast bootstrap approximation (UFBoot) and ModelFinder was used to select the best fit models of GTR+F+I+G4 and TIM3+F+I+G4 for SSU and LSU trees respectively.[48,49]

A phylogenomic analysis was performed by using 263 curated alignments of conserved genes as queries in a series of BLASTP searches.[50] Resulting hits were added to their respective alignments which were then trimmed in trimAl (80% gap threshold) and used to infer single gene trees with IQ-TREE (model: LG+G). Each tree was then visually inspected in FigTree v1.4.4 to remove contaminants, paralogs, and isoforms, leaving behind a maximum of one best representative sequence per transcriptome. Cleaned alignments were parsed using SCaFoS v4.55 to select the taxa and genes (those present in $\geq$60% of final taxa) that would be included in the analysis.[39] A maximum likelihood (ML) tree was inferred from the concatenated, parsed gene alignments using the model LG+C60+F+G4 and UFBoot. A Bayesian analysis was performed in four parallel runs on the same alignment in Phylobayes-MPI with the model CAT+GTR+G4.[40] Chains were allowed to run until they surpassed 10,000 iterations, at which point the first 10% of trees were removed as burn-in and a consensus tree was constructed from all parallel runs (available at https://doi.org/10.5281/zenodo.7269039).

Plastid protein search

Searches were performed against all transcriptomes for genes of plastid origin to confirm the presence of plastids and look for evidence of photosynthetic mechanisms. Among these were heme, isoprenoid, and iron-sulfur cluster pathway enzymes, which are typically found in non-photosynthetic taxa targeted from the nucleus to the reduced plastid.[18] Searches were also performed for photosynthesis related genes associated with photosystems II and I, cytochrome b_6f, plastoquinol oxidation, plastid electron transport (PET), light harvesting, ATP synthesis, cyclic electron flow (CEF), the Calvin cycle. Ribulose-1,5-bisphosphate carboxylase (RuBisCo) and phosphoribulokinase (PRK) were the only Calvin cycle genes included in this search because they are the only genes unique to this process. Other Calvin cycle genes were found to be present in both photosynthetic and heterotrophic lineages outside of the warnowiids and were therefore not reported here, as their presence is not indicative of Calvin cycle activity. A search for rhodopsin was performed using a curated alignment containing the putative *Erythropsidinium* homolog (BAQ59586.1), as well as for retinal synthesis pathway proteins, *crtB*, *crtI*, *crtY*, and *diox1*.[2,51] Protein import across the innermost membrane of the chloroplast (*TIC20*, *TIC110*) and the thylakoid membrane (*tatA*, *tatB*, *tatC*, *secA*, *secE*, *secY*) were also investigated in warnowiids.

All BLAST searches were performed with an e-value threshold of 1e^{-10}. Resulting BLAST hits were trimmed of extraneous sequence extensions and combined with their respective queries, aligned, and trimmed with an 80% gap threshold. Trees were inferred from trimmed alignments in IQ-TREE (model: LG+G) to differentiate relevant homologs from contaminants and paralogs. Trees were visually inspected for contaminants, which were removed from original alignments before realigning and trimming as described above, and producing the final single gene trees in IQ-TREE with UFBoot (model: LG+F+I+G4). Interpreting the presence and absence of retinal pathway components was difficult because their respective carotenoid products can be used in capacities other than rhodopsin-associated retinal synthesis. The phylogeny of *diox1* includes many homologous genes in the same family, the functions of which are not known, so only the closest clade of dinoflagellate homologs grouping with known retinal-producing *diox1* (BAA18428.1) were counted as present.

The N-termini of all warnowiid transcripts associated with PSII, cytochrome b_6f, PSI and ATP synthase, were inspected for plastid targeting signal peptides to determine if the presence and absence of these extensions correspond to the genes thought to be encoded in the nuclear and plastid genomes, respectively. First, transcripts were compared against prokaryotic sequences in alignments to determine if an N-terminal extension was present. When extensions were present, they were entered into SignalP v3.0 and visually inspected for the "FVAP" motif characteristic of dinoflagellate plastid targeting signals to confirm their identity.[18,31]

QUANTIFICATION AND STATISTICAL ANALYSIS

Statistical support for the ML phylogenetic tree was inferred using the model LG+C60+F+G4 and 1000 bootstrap replicates. Bayesian analysis was performed on the same alignment in four parallel runs with the model CAT+GTR+G4 in Phylobayes-MPI.[40]

Current Biology, Volume *33*

Supplemental Information

Photosystems in the eye-like organelles of heterotrophic warnowiid dinoflagellates

Elizabeth C. Cooney, Corey C. Holt, Victoria K.L. Jacko-Reynolds, Brian S. Leander, and Patrick J. Keeling

Current Biology, Volume *33*

Supplemental Information

Photosystems in the eye-like organelles of heterotrophic warnowiid dinoflagellates

Elizabeth C. Cooney, Corey C. Holt, Victoria K.L. Jacko-Reynolds, Brian S. Leander, and Patrick J. Keeling

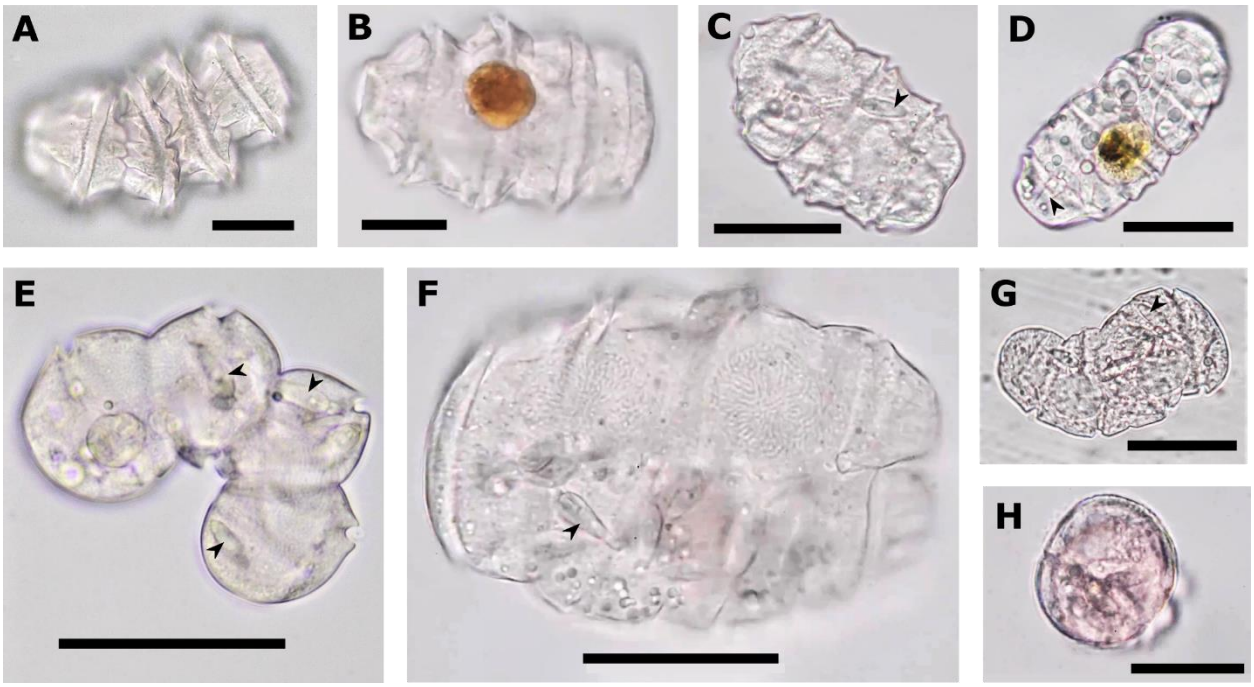

Figure S1: Light micrographs of polykrikoid cells, related to Figure 2. (A-H) *Polykrikos kofoidii* cells Pk-FC1:7 and Pk-QI8. Black arrows indicate visible nematocysts. Scale bars are 50 µm.

Figure S2: Single gene phylogenies for *atpF* and *psbO*, related to Figure 4. Orange branches indicate dinoflagellate clades. Warnowiid sequences are bold, with sequences collected in the present study indicated in cyan or grey. In *atpF*, grey branch labels indicate highly divergent sequences, while in *psbO*, they indicate likely contamination. Node values show bootstrap support, with values of 100 indicated by black circles. Trees were inferred from models selected with ModelFinder – *atpF*: LG+F+G4; *psbO*: LG+F+I+G4[S1]. Scale bars indicate the number of amino acid substitutions per site.

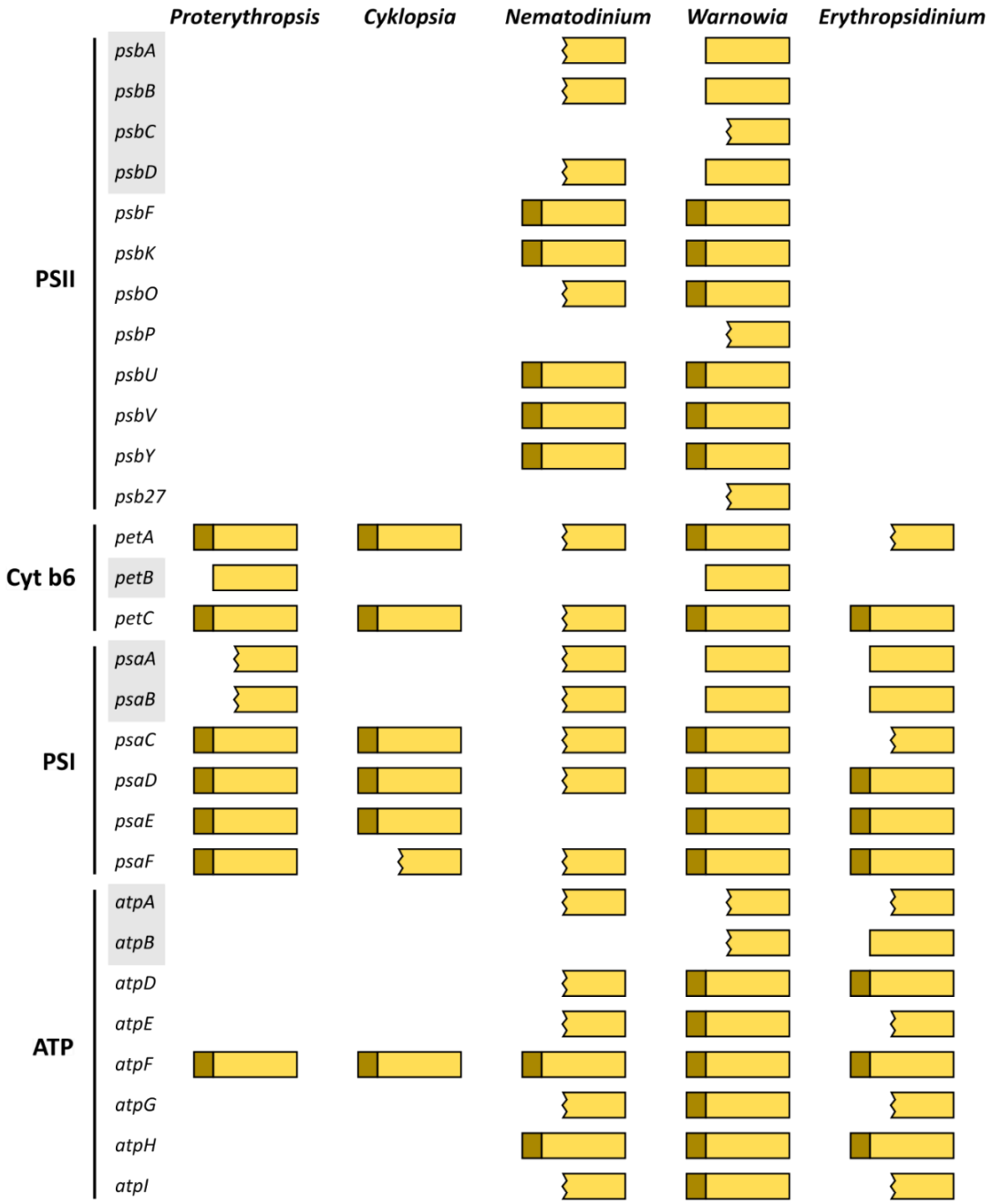

Figure S3: Signal peptide extensions on photosystems, cytochrome b6, and ATP synthase genes, related to Figure 4. Yellow bars represent the presence of at least one sequence in the transcriptomes of the corresponding genus. Strait leading edges indicate intact sequences while sequences with truncated N-termini where the presence of a signal could not be determined have jagged edges. Brown N-terminal caps indicate the presence of a plastid targeting signal peptide. Genes highlighted in grey are typically encoded in the dinoflagellate plastid genome.

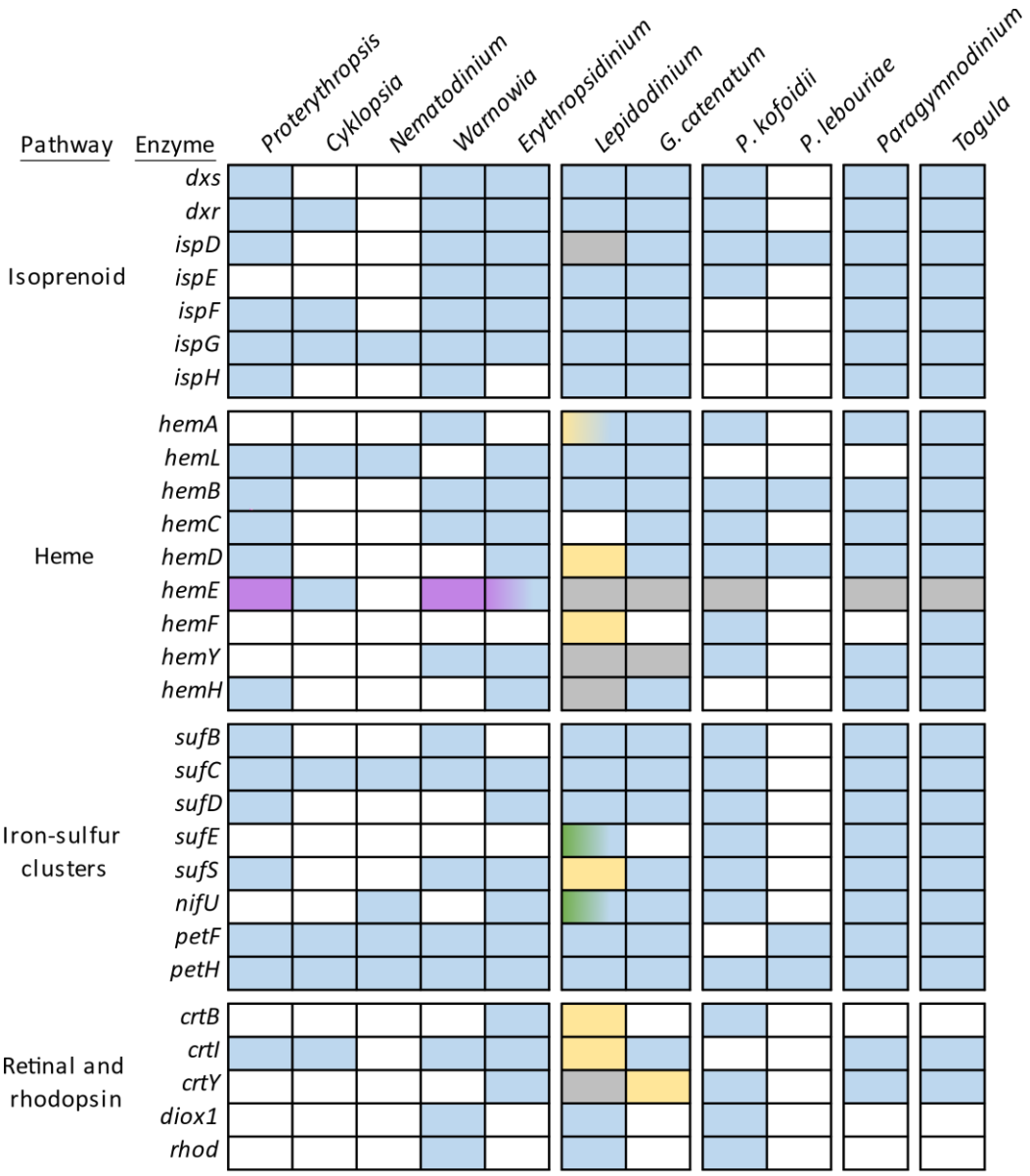

Figure S4: Presence of biosynthesis pathway genes, related to Figure 4. Fill indicates presence of isoprenoid, heme, and iron-sulfur cluster synthesis enzyme genes. Colors correspond to the gene origin: blue = ancestral peridinin plastid; yellow = stramenopile; green = green algae; purple = haptophyte; two colors = two homologs from different origins; grey = more than two homologs of different origins.

Taxon	ID	Date	Location	PR	PCS
Proterythropsis sp.	Pr-FC1	29-May-20	False Creek	13,125,649	23183
Proterythropsis sp.	Pr-FC2	10-Sep-20	False Creek	3,069,280	39149
Proterythropsis sp.	Pr-FC3	10-Sep-20	False Creek	1,971,256	18327
Proterythropsis sp.	Pr-FC4	10-Sep-20	False Creek	2,084,421	23,183
Proterythropsis sp.	Pr-QI5	06-Aug-21	Quadra Island	7,933,207	65478
Proterythropsis sp.	Pr-QI6	06-Aug-21	Quadra Island	9,953,653	16096
Proterythropsis sp.	Pr-QI7	06-Aug-21	Quadra Island	7,394,303	28654
Proterythropsis sp.	Pr-QI8	07-Aug-21	Quadra Island	7,459,341	8648
Cyklopsia gemma	Cy-JP1	29-Dec-20	Jericho Pier	14,034,730	66,009
Cyklopsia sp.	Cy-FC2	03-Feb-21	False Creek	22,837,615	21,081
Nematodinium sp.	Nm-QI1	15-Sep-21	Quadra Island	19,820,632	13,396
Nematodinium sp.	Nm-QI2	15-Sep-21	Quadra Island	13,301,809	24,665
Erythropsidinium sp.	Er-QI1	06-Aug-21	Quadra Island	4,740,668	39,709
Erythropsidinium sp.	Er-QI2	07-Aug-21	Quadra Island	7,782,366	58,379
Warnowia sp.	Wa-QI1	27-Jul-22	Quadra Island	18,919,413	34,697
Warnowia sp.	Wa-QI2	27-Jul-22	Quadra Island	8,112,544	21,811
Warnowia sp.	Wa-QI3	27-Jul-22	Quadra Island	7,113,298	26,597
Warnowia sp.	Wa-QI4	27-Jul-22	Quadra Island	7,248,892	23,585
Polykrikos kofoidii	Pk-FC1	06-Oct-20	False Creek	5,889,644	14,664
Polykrikos kofoidii	Pk-FC2	06-Oct-20	False Creek	7,945,958	14,335
Polykrikos kofoidii	Pk-FC3	06-Oct-20	False Creek	9,377,166	9,289
Polykrikos kofoidii	Pk-FC4	07-Nov-20	False Creek	14,080,417	12,220
Polykrikos kofoidii	Pk-FC5	22-Nov-20	False Creek	8,138,619	23,804
Polykrikos kofoidii	Pk-FC6	04-Dec-20	False Creek	7,813,634	14,386
Polykrikos kofoidii	Pk-FC7	04-Dec-20	False Creek	8,577,298	26,766
Polykrikos kofoidii	Pk-QI8	07-Aug-21	Quadra Island	7,950,172	26,813

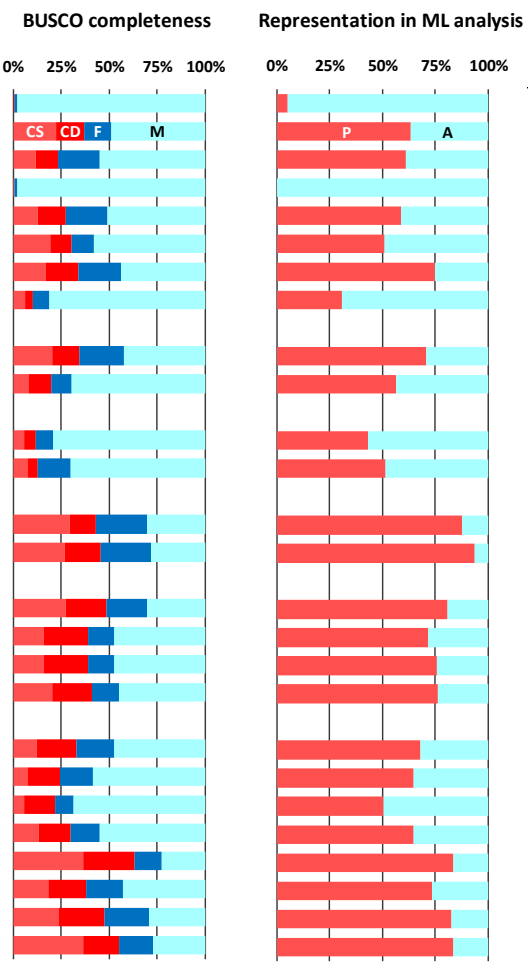

Table S1: Information and quality assessments for each single cell transcriptome, related to Figure 3. Dates and locations of each cell's collection are listed. ID = cell identifier; PR = number of paired reads; PCS = protein coding sequences. BUSCO completeness scores were estimated using the alveolata_odb10 database. CS = complete, single sequence; CD = complete, duplicated sequence; F = fragmented; M = missing. Representation in maximum likelihood (ML) analysis shows the percent of genes from the ML analysis present (P) and absent (A) in each transcriptome.

Supplemental reference

S1. Kalyaanamoorthy, S., Minh, B.Q., Wong, T.K.F., Von Haeseler, A., and Jermiin, L.S. (2017). ModelFinder: Fast model selection for accurate phylogenetic estimates. Nat. Methods *14*, 587–589. 10.1038/nmeth.4285.

Taxonomic summary
Class DINOPHYCEAE West & Fritch, 1927
Order GYMNODINIALES Lemmermann, 1910
Family WARNOWIACEAE Lindemann, 1928

Genus *Cyklopsia* gen. nov. Cooney, Leander, & Keeling, 2022
Diagnosis. An ocelloid-bearing sister branch to *Proterythropsis*. Cells are athecate, lacking pigment except for the retinal body of the ocelloid, and can have nematocyst-like extrusomes. In vegetative cells, ocelloids are positioned toward the posterior end inside the cell.
Type species. *Cyklopsia gemma* Cooney, Leander & Keeling 2021
Etymology. *Cyklopsia* is adapted from “Cyclops” or “Kýklōps”, a one-eyed monster from Greek mythology. “Cyclops” is a Latinized version of the original Greek name, which translates to “round eye”. This name is a reference to the single round ocelloid possessed by members of this genus. Gender is feminine.
Zoobank ID. 177EEA40-C4D4-4D34-8D9B-43D30413658B

***Cyklopsia gemma* sp. nov. Cooney, Leander, & Keeling, 2021**

Diagnosis. Unicellular ocelloid-bearing dinoflagellate. Cells are unpigmented (with the exception of the ocelloid) and approximately 40 µm in length. The episome of the cell is rounded and wider than the rest of the cell while the nucleus fills the anterior portion of the cell and the ocelloid is positioned in the posterior. Cells have a wing-like posterio-lateral extension.
Holotype. Cell Cy-JP1, seen in Fig. 1*I*.
Etymology. The Latin “gemma” means gem, referring to the ruby-like retinal body of the ocelloid. Gender is feminine.
Type locality. Collected from Jericho Pier in Vancouver, BC (49.276996, -123.201612). Collector: E. Cooney.
Sequence data. Raw reads: SRA (project number PRJNA922587). Single-cell transcriptome: https://doi.org/10.5061/dryad.nzs7h44vf. SSU rRNA gene sequence: OP604718. LSU rRNA gene sequence: OP604692.
Zoobank ID. 177EEA40-C4D4-4D34-8D9B-43D30413658B